The International Journal of Advanced Manufacturing Technology (2020) 111:325–339
https://doi.org/10.1007/s00170-020-06029-8

ORIGINAL ARTICLE

Printed and hybrid integrated electronics using bio-based and recycled materials—increasing sustainability with greener materials and technologies

Marja K. Välimäki[1] · Laura I. Sokka[2] · Heidi B. Peltola[3] · Sami S. Ihme[1] · Teijo M. J. Rokkonen[3] · Timo J. Kurkela[1] · Jyrki T. Ollila[1] · Arttu T. Korhonen[1] · Jukka T. Hast[1]

Received: 29 April 2020 / Accepted: 1 September 2020 / Published online: 26 September 2020

Abstract

Printed and hybrid integrated electronics produced from recycled and renewable materials can reduce the depletion of limited material resources while obtaining energy savings in small electronic applications and their energy storage. In this work, bio-based poly(lactic acid) (PLA) and recycled polyethylene terephthalate (rPET) were fabricated in film extrusion process and utilized as a substrate in ultra-thin organic photovoltaics (OPV). In the device structure, metals and metal oxides were replaced by printing PEDOT:PSS, carbon and amino acid/heterocycles. Scalable, energy-efficient fabrication of solar cells resulted in efficiencies up to 6.9% under indoor light. Furthermore, virgin-PET was replaced with PLA and rPET in printed and hybrid integrated electronics where surface-mount devices (SMD) were die-bonded onto silver-printed PLA and virgin-PET films to prepare LED foils followed by an overmoulding process using the rPET and PLA. As a result, higher relative adhesion of PLA-PLA interface was obtained in comparison with rPET-PET interface. The obtained results are encouraging from the point of utilization of scalable manufacturing technologies and natural/recycled materials in printed and hybrid integrated electronics. Assessment showed a considerable decrease in carbon footprint, about 10–85%, mainly achieved through replacing of silver, virgin-PET and modifying solar cell structure. In outdoor light, the materials with low carbon footprint can decrease energy payback times (EPBT) from ca. 250 days to under 10 days. In indoor energy harvesting, it is possible to achieve EPBT of less than 1 year. The structures produced and studied herein have a high potential of providing sustainable energy solutions for example in IoT-related technologies.

Keywords Printed electronics manufacturing · Printed solar cells · Poly(lactic acid) · Recycled PET · Life cycle assessment · Climate impacts

1 Introduction

Limiting the average global warming to well below 2° in comparison with pre-industrial times calls for drastic reductions in the global greenhouse gas emissions within the next decades. Sustainable use of material resources and full-scale utilization of renewable energy are among the key solutions for limiting of greenhouse gas emissions. In this respect, the European Commission has adopted an Ecodesign directive to improve the environmental performance of products through the product-specific regulations [1]. Transition from the excess consumption of fossil-based materials and energy towards technologies based on sustainable and safe materials needs to take place. Furthermore, the low utilization of side/waste stream materials has to be improved.

Electronic supplementary material The online version of this article (https://doi.org/10.1007/s00170-020-06029-8) contains supplementary material, which is available to authorized users.

✉ Marja K. Välimäki
Marja.Valimaki@vtt.fi

[1] VTT Technical Research Centre of Finland, Kaitoväylä 1, P.O. Box 1100, FI-90571 Oulu, Finland

[2] VTT Technical Research Centre of Finland, Vuorimiehentie 3, P.O. Box 1000, FI-02150 Espoo, Finland

[3] VTT Technical Research Centre of Finland, Visiokatu 4, P.O. Box PL 1300, FI-33720 Tampere, Finland

According to Cisco, 50 billion devices from smart wearables to smart cities and from households to industries will be connected to the Internet by 2020 [2]. From the consumption point of view, more off-grid energy will be needed especially as the use of gadgets and mobile devices keep on increasing. The known lithium reserves are likely not enough to satisfy the growing demand of batteries, so energy-autonomous solutions have to be implemented. The predicted market growth for batteries and accumulators is so high that inadequate resource availability could become a limitation even with efficient recycling [3]. Therefore, alternative and supplementary sources of energy are needed.

Solar energy technologies provide an excellent opportunity to address the challenges mentioned above. Replacement of conventional fossil energy sources through solar power is one of the key technologies for climate change mitigation. Furthermore, solar energy has limitless potential in providing electricity in different environments and, it is available for everyone, everywhere. Printed and hybrid integrated devices provide opportunities such as material and energy savings, among others [4–7]. Manufacturing technologies that are currently being implemented allow decreased material consumption up to 75%, mainly by reducing the use of plastics and PCBs [8].

Organic photovoltaics (OPV) have obtained power conversion efficiencies (PCE) up to 17% under solar irradiation and up to 28% under indoor light conditions [9, 10]. Systems with energy-autonomous devices have the potential of replacing disposable batteries. Fabricating the lightweight, flexible and ultra-thin devices using printing technologies enables extremely low consumption of materials and further eliminates energy-intensive inert or vacuum stages, by replacing them with processes that can take place at ambient condition [11–13]. Overmoulding of printed and hybrid integrated systems using injection moulding leads to 50–70% lighter devices and up to 90% thinner thermoplastic-electronic devices [8]. Carbon footprint values of 20.7 kg CO_2eq./m^2 have been presented for ITO-free OPV processes in the literature [14]. This translates into 55.1–92.8 g CO_2eq./kWh electricity, which is considerably lower than for example the emission factor for natural gas (approximately 200 g CO_2eq./kWh electricity). In a study by Tsang et al., energy payback times (EPBT) of OPVs were found to lie between 220 and 460 days depending on the application scenario, thus being 50–60% lower than those of the amorphous silicon panels in the same study [15].

Organic electronics enable exploiting device materials extracted from nature or synthetic derivatives of natural molecules. Steps has been taken towards using materials such as pigments like indigo, ß-carotene, cellulose and its derivates and small molecules like amino acids or peptides, e.g. in transistors and solar cells as a semiconductor, dielectric or interfacial layer [16–25]. Until now, polyethylene terephthalate (PET), polyethylene napthalate (PEN), polycarbonate (PC) and polyimide (PI) have been the most common substrate material used in printed and hybrid integrated electronics [26–28]. Success of PET has been based on optical transparency, dimensional stability at higher temperatures, solvent resistance, flexibility and affordability of the price [27, 28]. The choice of substrate is relevant since the substrate can comprise 40–80% of the weight or volume of entire thin film device [11, 29].

Within bio-based alternatives, silk, gelatin, natural resin shellac and cellulose-based papers are one possibility to exploit [19, 24, 30]. Solar cells have been fabricated on top of paper, coated with polymer or glue with an efficiency of 3–4% [31, 32]. However, the surface roughness, lack of transparency, barrier properties and moisture resistance are limiting the use of paper substrates. Another alternative is to replace PET substrate with cellulose nanofiber films to obtain optically and mechanically high-quality film with desired barrier properties [33–35]. PCE of 1.4% was reported when OPV was prepared directly on nanocellulose film and 4.25% when perovskite solar cell was prepared on nanocellulose film with acrylic coating [36, 37]. In polymeric solutions, the approaches to utilize bio-based polymers as substrate material have focused on transfer strategies where the device or part of it has first been prepared on different substrate, or by coating the polymeric material on top of another substrate [19, 30, 38]. Within bio-based polymers, poly(lactic acid) (PLA) is one of the most promising material. It is stiff, transparent and commercially available in various grades. However, due to its low heat resistance and slow crystallization rate, the use of PLA in printed electronics instead of PET is challenging. Increased crystallization, and thus improved mechanical performance and heat resistance of PLA, can be achieved, e.g. by nucleation, strain-induced crystallization through orientation or stereocomplex blends [39–41].

In contrast to biodegradability and disposability, recycled polymers provide an environmentally friendly alternative to conventional polymers by saving virgin raw material resources, thus contributing to a circular economy and detaching from fossil dependency [42]. Among the recycled polymers, PET derived from post-consumer bottles is one of the few recycled plastics available in commercial scale with high quality [42].

The aim of this work was to reduce, replace and reuse materials in renewable energy production and in electronics while still maintaining or even improving the functionality of the technology. In this work, the use of virgin raw materials was minimized by replacing fossil-based materials with recycled and bio-based alternatives. Recycled PET (rPET) and PLA thin films were prepared in cast film extrusion process and used as a substrate in the preparation of printed and hybrid integrated electronic devices. OPV structures for energy harvesting under indoor light conditions were printed on

PET, rPET and PLA substrates. The alternatives to replace sputtering process and wet deposition of metal oxides and metals was realized by gravure and screen printing PEDOT:PSS, amino acid/heterocycles, e.g. histidine and carbon. In the processing of printed and hybrid integrated electronics, surface-mount devices (SMD) were die bonded onto silver-printed PLA and virgin-PET films to produce LED foils followed by an overmoulding with rPET and PLA. In order to assess the impact of these changes on the carbon footprint and energy consumption of printed OPV with selected device structures on rPET, PLA and polyethylene furanoate (PEF) substrates in comparison with a reference structure based on virgin-PET, a life cycle assessment (LCA) methodology was used.

2 Experimental section

2.1 Materials and methods for production of sustainable printed devices

Two different materials were selected to produce substrates for printed and hybrid integrated devices: recycled PET and bio-based PLA. High-quality Pramia rPET food-grade GR granulates made from PET bottles obtained through Finnish bottle recycling system were purchased from Pramia Plastic Oy, Finland. High-viscosity Luminy LX175 PLA homopolymer suitable for film extrusion was purchased from Total Corbion PLA BV. rPET and PLA grades were obtained as crystalline white pellets, having densities of 1.4 and 1.24 g/cm^3, glass transition temperatures of 78–82 °C and 55–60 °C and melting points of 245 and 155 °C, respectively.

The laboratory-scale fabrication of rPET and PLA substrates was performed with Brabender Plastograph EC Plus 19 mm single screw extruder with 120 mm cast film die. For rPET, the temperature profile was 280–290–280–280 °C from zone 1 to die, with a screw speed of 26–27 rpm. The film was extruded onto a chill roll having temperature of 83–84 °C and processed into cast films through calenders to a final film thickness of 200 μm (unoriented films) or 360–400 μm (films for biaxial orientation). For PLA, the temperature profile was 240–230–230–220 °C from zone 1 to die, with a screw speed of 50 rpm. The chill roll temperature was 48 °C and the final film thickness before biaxial orientation was approximately 750 μm.

Part of the produced cast film was biaxially oriented to achieve lower film thickness and improved mechanical properties. Biaxial orientation was performed with biaxial laboratory stretcher (Brückner Karo IV). The used parameters for rPET were the following: preheating time 100 s, temperature 91 °C, orientation ratio 2.4 × 2.4, final thickness 60–70 μm. For PLA, the orientation preheating temperature and time was 75 °C for 120 s and orientation ratio was 3.2 × 3.2. PLA films were heat stabilized after orientation in oven at 140 °C for 4 min. The final film thickness was 60–70 μm.

Pilot-scale rPET film was prepared with a 550-mm-wide cast film extrusion line (Extron-Mecanor Oy). The material was processed with starve-fed 35 mm single-screw extruder equipped with a melt pump (Extron-Mecanor Oy). The temperature in all zones from zone 1 to die was 290 °C. Screen pack of 80–50 mesh was used. Material consumption was approximately 10 kg/h, and the chill roll temperature was 15 °C. The cast film was oriented online in machine direction (MD) with in-house-designed MD orientation unit, and the orientation ratio in MD was 3×. The film was preheated at 90 °C and annealed online at 150–160 °C after orientation. The oriented film thickness was 50–70 μm.

OPV devices were prepared on rPET and PLA substrates, commercial PET (Melinex ST506, DuPont Teijin Films, USA) and indium tin oxide (ITO)-coated PET (40–60Ωsq, Eastman, USA) were used as a reference substrate. Different configurations were prepared according to the plan presented in Fig. 1.

Both poly-(3,4-ethylenedioxythiophene):poly (styrenesulfonate) (PEDOT:PSS) inks were prepared by mixing PEDOT:PSS (Clevios PH1000, Heraeus, Germany), isopropyl alcohol (IPA) and either ethylene glycol (EG) or dimethyl sulfoxide (DMSO) with a ratio of 73:22:5 per weight. Fifty- and 90-nm-thick layers of PEDOT:PSS were gravure-printed directly on top of PET, rPET and PLA substrates (Labratester, Norbert Schläfli Maschinen, Switzerland). 2-Hydroxypyridine, glycine and histidine (Sigma-Aldrich, Germany) were dissolved into the mixture of ethanol and DI-water (1:1) in 1 mg/ml concentration. In addition, histidine was prepared in 0.1, 0.2 and 0.5 mg/ml concentration. Preparation of zinc oxide (ZnO) and poly-(3-hexylthiophene):[6,6]-phenyl C61 butyric acid methyl ester (P3HT:PCBM) was carried out as reported in the paper by Apilo et al. [43]. However, maximum processing temperatures were 120 °C for PET, 60 °C for rPET and 100 °C for PLA. Gravure-printed 2-hydroxypyridine, histidine and glycine layers on ITO-PET were dried at 50 °C for 5 min. Standard devices comprised 1 nm of LiF and 100 nm of Al on top of solar cell and, 100 nm of Ag on top of bottom electrode contact through thermal evaporation. Respectively, inverted devices comprised 1 nm of MoO_3 and 100 nm of Ag or screen-printed PEDOT:PSS (EL-P 5015, Agfa, Belgium) and carbon paste (PF-407A, Henkel, Germany).

Printed and hybrid integrated LED foils were prepared through screen printing and die-bonding processes on PLA substrate, and the commercial PET was the reference substrate. Ag conductors were screen printed with Ag paste (LS-411 AW, Asahi, Japan) on PLA and PET (Melinex ST506, DuPont Teijin Films, USA) substrates using a flat-bed sheet-to-sheet screen printer (EKRA XH STS, ASYS Group, Germany). Films were dried in an oven at 80 °C for 30 min. Die-bonding of LEDs was made with thermally and electrically conductive epoxy (EpoTek H20E, Epoxy Technologies, USA) and curing at

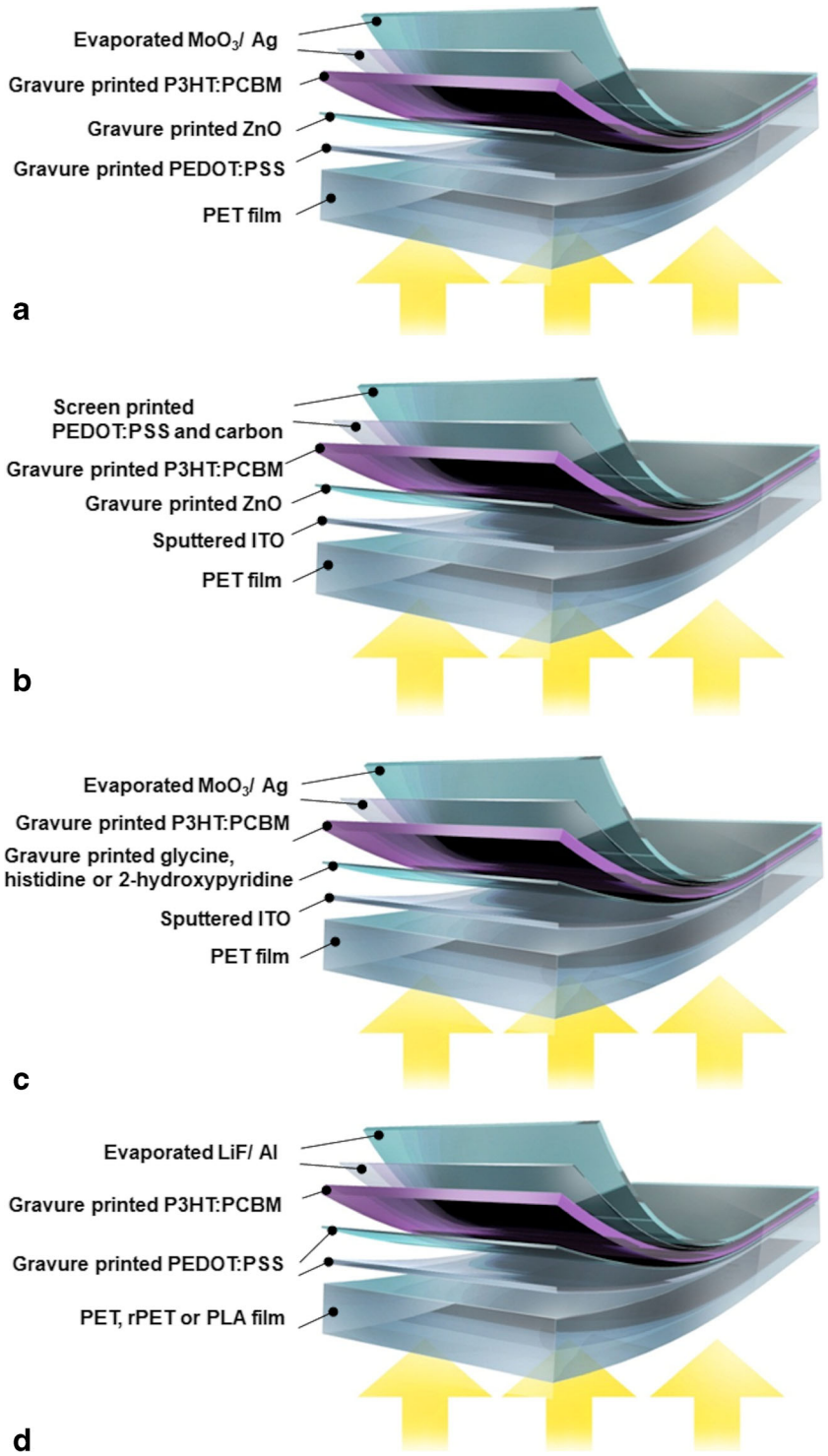

Fig. 1 Fabrication of following printed organic solar cell structures: inverted device configurations comprising **a** gravure-printed PEDOT:PSS electron contact, **b** screen-printed carbon hole contact, **c** gravure-printed amino acid/heterocycle electron injection layer and **d** standard device configuration on PET, rPET and PLA film

80 °C. To improve the mechanical support, UV-curing adhesive (Loctite 3525, Henkel, Germany) was dispensed around each LED.

To seal optical and mechanical functionalities, the printed and hybrid integrated electronics foil was overmoulded [7]. This injection moulding process is typically called as injection moulded structural electronics (IMSE™), which is a low-cost manufacturing technology especially for high production volumes. Here, hydraulic injection moulding machine (Engel Victory 120 Duo, Engel, Austria) was used for overmoulding experiments. The overmoulding parameters were specified experimentally for good mould filling and part quality. The selected parameters and the test part are presented in Fig. 2.

The tensile strength of commercial PET and PLA foils was specified according to the ISO 527-3 for a reference to the adhesion strength. The adhesion between the foil and overmoulding material was evaluated with a lap shear test with the tensile rate of 10 mm/min. The testing setup was not a pure shear test due to the curvature sample geometry; thus, in addition to the shear strength values, the tensile strength values were also specified for better accuracy and comparability with the reference tensile strength values of the foils. The lap shear test setup is shown in Fig. 3.

2.2 Characterization methods and equipment

Light transmission was measured using a UV-Vis-NIR Spectrometer (Varian Cary 5000, Agilent, USA), layer thickness using a profilometer (Dektak, Veeco, USA) and sheet resistance using a Keithley 2400 source-meter (Keithley Instruments, USA). The current–voltage (I-V) measurements under solar irradiation were carried out using an AM1.5 solar simulator (SolarTest 1200, Atlas, USA), calibrated to 100 mW/cm^2 (Si-reference cell filtered with a KG5 filter). The I-V measurements performed under indoor light conditions were carried out using light cabin (Pantone, USA) with applied LED light (Nichia_3800K.int, Nichia, Japan). The irradiance (mW/cm^2) of the LED light at 200 lx and 1000 lx was calculated by measuring the light spectrum and lux levels with illuminance spectrophotometer (CL-500A, Konica Minolta, Japan).

a.)

Parameter	PLA	rPET
Injection pressure [bar]	413	260
Injection time [s]	2,3	1,7
Holding pressure [bar]	400	180
Holding time [s]	4	6
Melt temperature [°C]	200	270
Mold temperature [°C]	35	30
Cooling time [s]	30	40

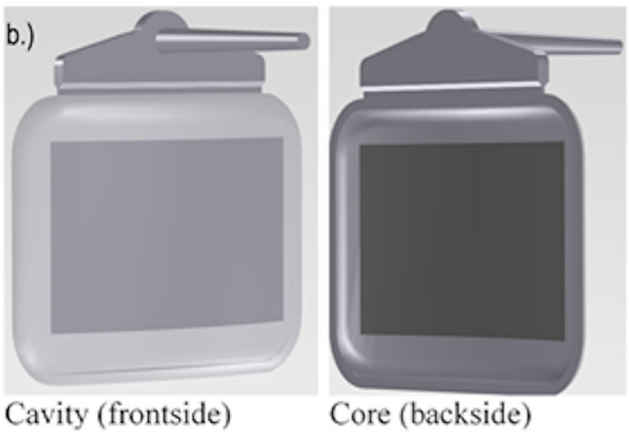

Fig. 2 Selected **a** injection moulding parameters for rPET and PLA and **b** overmoulding test part, where the cavity is a concave side of mould half plate and the core is a convex side of mould half plate

2.3 Life cycle assessment: methodology and materials

Life cycle assessment is a method for assessing the environmental impacts of product, service or system throughout its life cycle [44]. Through the assessment, a comprehensive understanding of the environmental impacts of the product can be established [45, 46]. Life cycle assessment is based on two standards: ISO 14040:2006 (Environmental Management–Life Cycle Assessment–Principles and Framework) [47] and ISO 14044:2006 (Environmental Management–Life Cycle Assessment–Requirements and Guidelines) [48]. The two standards complement one another, with ISO14041 providing the overview of the operation, applications and limitations of LCA while ISO 14044 goes into more detail, giving guidance on data collection, life cycle impact assessment (LCIA) and interpretation of LCA results. There is also a further standard on carbon footprint, the ISO 14067 [49]. In this study, LCA was applied to assess the impacts of climate change and cumulative energy demand (CED) of six alternative structures (Table 1). The selection of materials was based on material availability and compatibility for printing processes. In structure 5, PEF was studied as an alternative substrate material. For CED, both demand of fossil energy and total energy demand were calculated. In addition, resource use and waste production were qualitatively studied. It should, thus, be emphasized that the analysis conducted was not a full LCA but was limited to quantitative study of two impact categories (climate change impacts and CED). In addition, energy payback time (EPBT) was calculated (see, e.g. [50]). EPBT refers to the time required for OPV system to produce the same amount of electricity (converted into equivalent primary energy) as the energy consumed over its life cycle.

Data used in LCA was based on different LCA databases, including the ecoinvent database and ELCD database, scientific papers and other LCA studies [51]. Table S1 detailing the references used for each process is included in the Supporting Information. Only the production of raw materials was included in the assessment. The printing phase was excluded from the study since it took place on a laboratory scale, which was considered as unrepresentative. Furthermore, it was estimated that its environmental burden would be similar for all the structures.

In the assessment of climate impacts, the global warming potentials as stipulated by the Intergovernmental Panel on

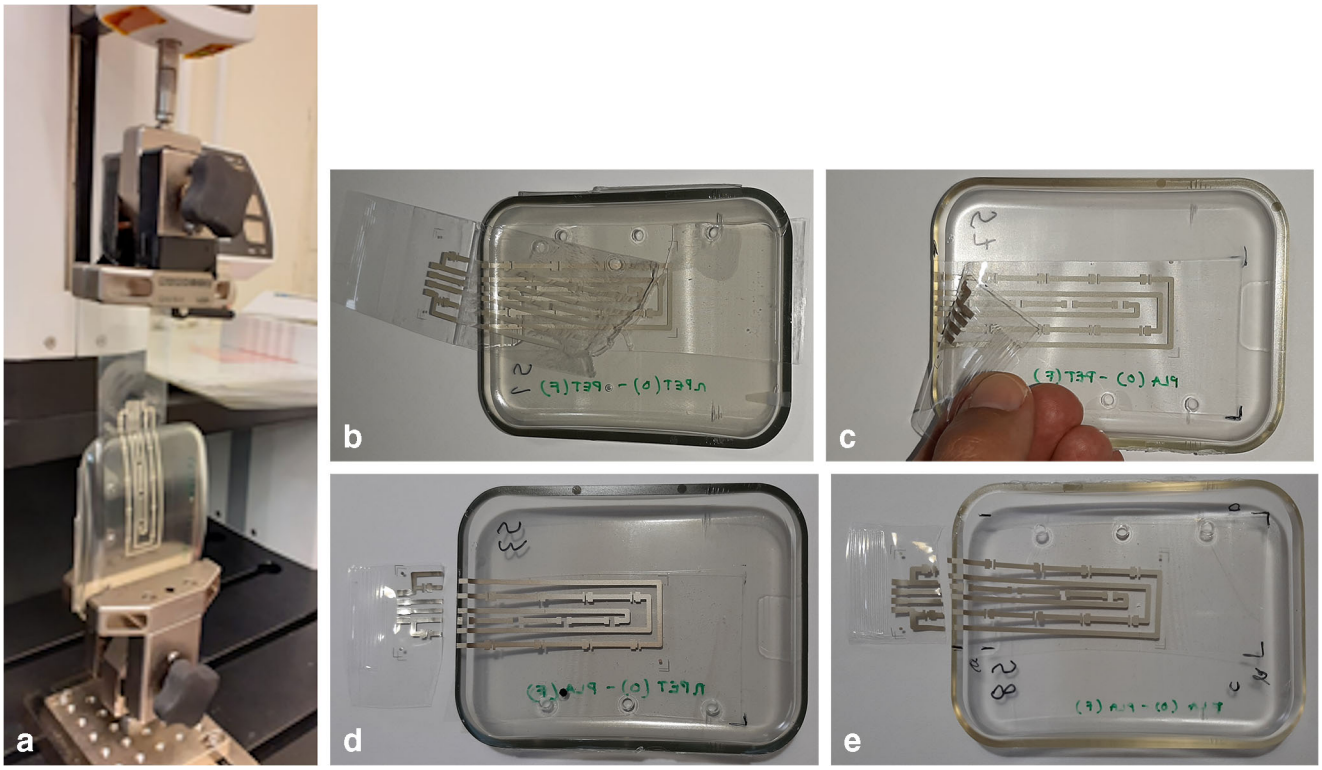

Fig. 3 **a** Lap shear test setup for the adhesion testing and, samples **b** PET(film)-rPET(overmoulding), **c** PET-PLA, **d** PLA-rPET and **e** PLA-PLA after lap shear test

Climate Change were used [52]. The assessment was conducted per m^2 of solar cell and per kWh of energy produced in both indoor and outdoor light conditions. For outdoor conditions, the annual sum of solar irradiation was assumed to be 1150 kWh/m^2 (representing Central European conditions). For indoor light conditions, 1 lux level of lighting (700) with 4000 use-hours per year was assumed. This would represent conditions in a very well-lighted environment, such as a supermarket or a mechanical workshop [53, 54]. Particularly for indoor light conditions, the assumptions are simplifications, as the level of lighting varies from one part of the room to another throughout the day, depending on the distance to the lighting unit, size of the windows, amount of daylight entering the room, season, etc. Here, the production efficiencies were assumed to be 3, 5 and 10% and lifetimes 10 and 20 years under outdoor and indoor light conditions. However, it should be noted that the production efficiencies and lifetimes under outdoor and indoor conditions might not be reachable with all assessed structures.

Table 1 Six different OPV structures (incl. materials and layer thickness) studied in the LCA

OPV structure	1 (ref.)	2	3	4, 5, 6		
Substrate 50 µm	PET	PET	r-PET	rPET	PEF	PLA
Hole/ electron contact	ITO 0.1 µm	Ag grid (30%) - PEDOT:PSS 0.2 µm -1 µm		PEDOT:PSS 0.05 µm		
Electron transport layer	ZnO-np 0.03 µm			Histidine 0.003 µm		
Photoactive layer	P3HT:PCBM 0.2 µm					
Hole transport layer	PEDOT:PSS 1 µm					
Hole/ electron contact	Ag 13 µm	Ag grid (30%) 13 µm		Biochar 8 µm		

3 Results and discussion

3.1 Assessment of printed devices and manufacturing

OPV devices were prepared on virgin-PET (commercial), rPET and PLA substrate films. All films reached the light transmission of 90% (Fig. S2, Supporting Information). PEDOT:PSS was gravure printed to replace sputtered hole/electron contact (bottom electrode), e.g. ITO, and screen-printed carbon to replace screen-printed Ag hole contact (top electrode). The use of metal oxides, e.g. ZnO, or polymers, e.g. PEIE, was replaced in electron transporting by gravure printing amino acid/heterocycles instead.

To assess the energy-harvesting abilities of described OPV structures for small, low-power autonomous energy systems, the work comprised device characterization under indoor light conditions. Indoor lighting conditions, typically ranging from

200 to 1000 lx and having 500–1000 times lower intensity than under solar irradiation at 1 sun (100 mW/cm^2) [55]. P3HT:PCBM-based OPV have reached 12.8% efficiency under LED light at 0.5–1 mW/cm^2 light intensity [56]. In efficient power conversion, low serial resistance (R_S) is preventing from power losses and high shunt resistance (R_{SH}) from unwanted current leakage. However, under low light intensities, the generated current is small and R_S becomes less significant [57]. Thus, under low light conditions, it is possible to have electrode materials with higher sheet resistance and print thin layer of PEDOT:PSS to replace, e.g. sputtered ITO. Cho et al. have resulted a sheet resistance of 359 Ω/□ů and a PCE of 2.0% for OPV under 100 mW/cm^2 solar irradiation (AM1.5 solar simulator) by using 100-nm-thick gravure-printed PEDOT:PSS with dimethyl sulfoxide (DMSO) on PET substrate [58]. In this work, 90-nm- and 50-nm-thick gravure-printed layers of PEDOT:PSS with DMSO and IPA reached a sheet resistance of 253 Ω/□ů (90 nm) and 386 Ω/□ů (50 nm). The replacement of DMSO with EG resulted in more uniform printing quality and a sheet resistance of 244 Ω/□ů (90 nm) and 461 Ω/□ů (50 nm); thus, PEDOT:PSS with EG was selected as a hole/electron contact material for OPV.

Devices with 90-nm-thick printed PEDOT:PSS on PET indicated low leakage current based on high R_{SH} (Table 2). Open circuit voltage (V_{oc}) remain high under indoor light conditions also at low light intensity, thus reaching 0.46 V at 1000 lx and 0.41 V at 200 lx. The obtained 0.69 fill factor (FF) reached significantly higher FF in comparison with the reported spin-coated P3HT:PCBM-based devices on ITO-glass under indoor light conditions [59, 60].

The 90-nm PEDOT:PSS on PET comprised the highest R_{SH} and the replacement of PET with PLA and rPET decreased R_{SH}. The reduction of performance was expected since PET was processed at 120 °C and, respectively, PLA at 100 °C and rPET at 60 °C. According to Steim et al., the decrease of R_{SH} below 2 kΩ cm^2 is expected to cause a sharp drop of V_{oc} when the light intensity is less than 1/10 of solar irradiation (at 1 sun) [55]. In this work, prepared structures on different substrates reached R_{SH} above 2 kΩ cm^2 and maintained high V_{oc} when were illuminated under higher and lower light intensities. Same device configuration prepared on PET, PLA and rPET resulted in 6.9%, 3.5 % and 2.6% efficiencies due to the differences in current and fill factor (Fig. 4). In the preparation of OPV, the drying conditions were the main differentiating factor between the commercial heat-stabilized PET substrate and the produced PLA and rPET substrates. The obtained results show that thin, flexible and transparent PLA and rPET are suitable substrate alternatives for printed thin film devices. Virgin-PET substrate is possible to replace with PLA and rPET substrate and, the thermal stability is possible to improve by optimizing the film extrusion process.

Aqueous solutions of glycine, 2-hydroxy pyridine and histidine were gravure printed on top of patterned ITO, all in 1 mg/ml concentration. In addition, histidine was gravure printed in 0.1, 0.2 and 0.5 mg/ml concentration. Depending on solid concentration of ink, the low-viscosity ink transfer was estimated to form in gravure printing process layer thickness ranging from 1 to 10 nm. J–V characteristics in Fig. 5 show that the fabrication of glycine, 2-hydroxy pyridine and histidine buffer layers are scalable for gravure printing process despite of the low layer thickness target. The highest V_{oc} of 0.59 V and a short circuit current (J_{sc}) of 8.1 mA/cm^2 was obtained by gravure printing 0.5 mg/ml histidine, whereas 0.2 and 0.1 mg/ml devices were leaking and indicating a lack of reproducibility.

Printed and hybrid integrated LED foils were prepared by die bonding the SMD components on PLA and commercial virgin-PET substrates with screen-printed silver conductors. Printed silver conductors on PLA and commercial virgin-PET substrates obtained 0.03 Ω/□ sheet resistance. Overmoulding with rPET and PLA sealed LED foils. The processing and handling of PLA film was comparable to commercial virgin-PET, and all bonded LEDs on PLA were functional (Fig. S3). The thermal stability was the main identified difference in the processing of PLA and PET substrate. Both the PLA and rPET had an amorphous structure and from the point of pre-drying, handling and overmoulding, the processing of PLA and rPET was similar to the processing of fossil-based commodity and engineering thermoplastics. Furthermore, the PLA film with printed Ag conductors and die-bonded SMD components were able to withstand the conditions of the injection moulding process, namely high pressure, temperature and shear stress (Fig. 6).

Table 2 Electrical properties of printed OPV prepared on PET, recycled PET and PLA substrate and measured under 1000 lx (first value) and 200 lx using LED light source for illumination

Front electrode-substrate device architecture	V_{oc} (V)	J_{sc} (μA/cm^2)	FF	PCE (%)	R_{SH}A (kΩ cm^2)	R_SA (kΩ cm^2)
PEDOT:PSS(50 nm)-PET (STD)	0.46; 0.42	65.61; 14.55	0.69; 0.69	5.90; 5.90	147; 202	76; 76
PEDOT:PSS(50 nm)-PET (INV)	0.47; 0.42	64.39; 14.59	0.65; 0.61	5.52; 5.21	57; 72	114; 115
PEDOT:PSS(90 nm)-PET (STD)	0.46; 0.41	80.74; 15.25	0.66; 0.67	6.89; 5.85	240; 1008	89; 121
PEDOT:PSS(90 nm)-PLA (STD)	0.45; 0.40	53.61; 10.23	0.52; 0.59	3.52; 3.39	36; 59	89; 645
PEDOT:PSS(90 nm)-rPET (STD)	0.42; 0.35	40.29; 8.58	0.55; 0.45	2.64: 1.97	6; 7	75; 75

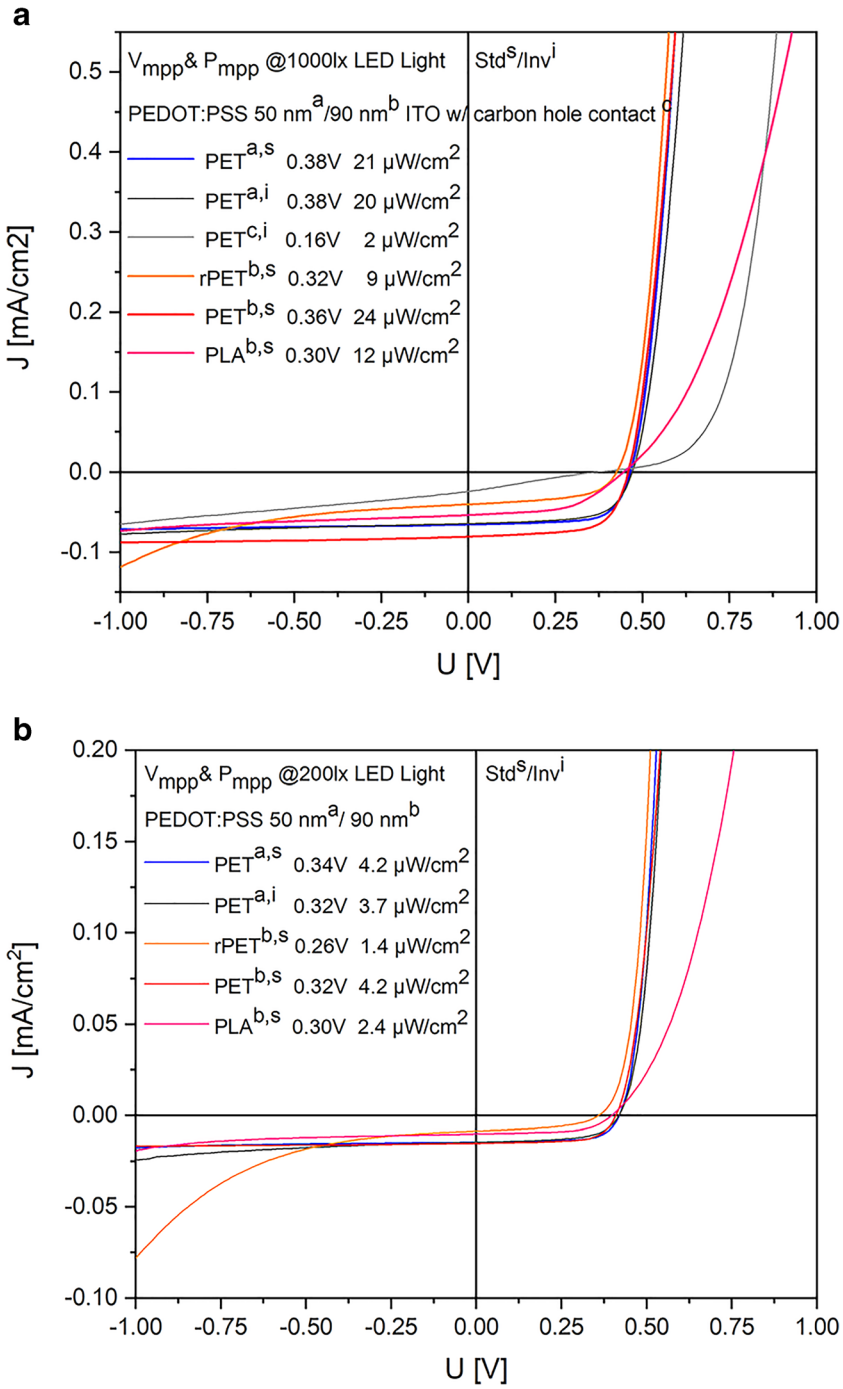

Fig. 4 J–V characteristics of printed solar cells prepared on PET, rPET and PLA substrate and measured at **a** 1000 lx and **b** 200 lx under illumination of LED light source

The tensile strength of the commercial PET and PLA foil materials were used as reference values. The tensile strength was specified in the tensile test with 10 parallel samples and, the reported average values and standard deviation are shown in Fig. 7. The tensile strength of the foils were specified also in the lap shear test, to be compared with the maximum tensile strength (Fig. 7), which indicates the adhesion strength in Fig. 8.

All the samples had a good adhesion due to the chemical compatibility between the foil and overmoulding material. The tensile strength of the lap shear test < the maximum tensile strength indicated adhesive type of the failure mechanism. The tensile strength of the lap shear test ≥ the maximum tensile strength indicated cohesive type of failure mechanism that was the case in (7), (8) and (9) PLA-PLA samples. It was concluded that PLA foils had better conditions for the adhesion most probably because of the lower Tg temperature. The shear stress values are shown in Fig. 9.

The shear stress values of the all samples indicated good adhesion even that was not able to state such as without the

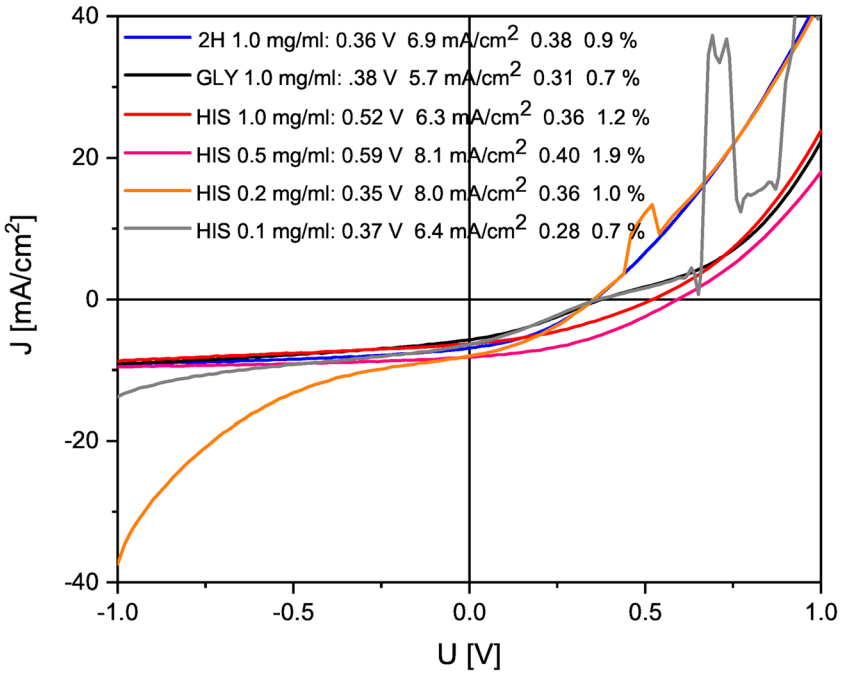

Fig. 5 J–V characteristics of OPVs measured under AM1.5 at 100 mW/cm^2 solar irradiation comprising gravure-printed glycine (Gly), 2-hydroxypyridine (2-H) and histidine (His) as electron transport layer

tensile strength values in the previous chapter. The rPET-PET combinations had higher shear stress due to the higher specific tensile strength of the foil even the relative adhesion of PLA-PLA samples were higher (Fig. 9). The obtained results are encouraging from the point of utilization of scalable manufacturing techniques and natural/recycled materials in printed and hybrid integrated electronics.

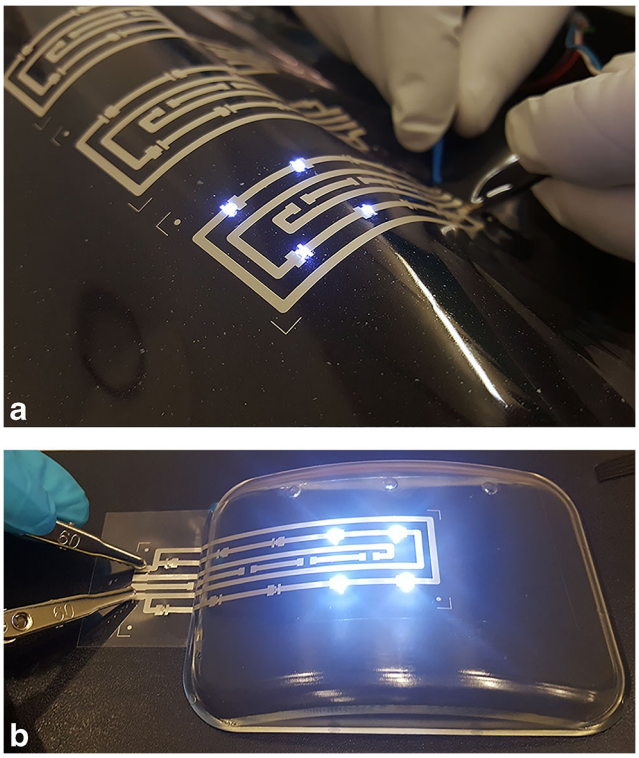

Fig. 6 Printed and hybrid integrated LED foils prepared on **a** PLA film and **b** overmoulded with rPET

3.2 Reduction of CO_2 emissions

Based on the assessment conducted in this study, all the structures studied had lower carbon footprint than the reference structure (Fig. 10) with fossil-based virgin-PET having the highest climate impact, followed by PLA and PEF. Among the substrate materials used, rPET had the lowest climate impact. Of the other materials, Ag and ITO contributed to most to the emissions. Thus, structure 4 resulted in the lowest overall emissions because it had rPET as the substrate material and no Ag paste.

3.3 Cumulative energy demand

Differences in the CED (MJ/m^2) of the different structures were similar to those of greenhouse gas emissions (GHG), as seen in Fig. 11. However, the cumulative CED of structure 6 was higher than that of structure 5. In structure 6, CED mainly resulted from production of PLA.

3.4 Extension of lifetime

Climate impacts and CED were also calculated per kWh of energy produced with the OPV structure (see Figs. S4–S6 in the Supporting Information). According to the results, outdoors GHG emissions ranged from ca. 30 g CO_2eq./kWh in the reference structure to less than 1 g CO_2eq./kWh in structures 4–6 (10% efficiency and 10 years lifetime). In

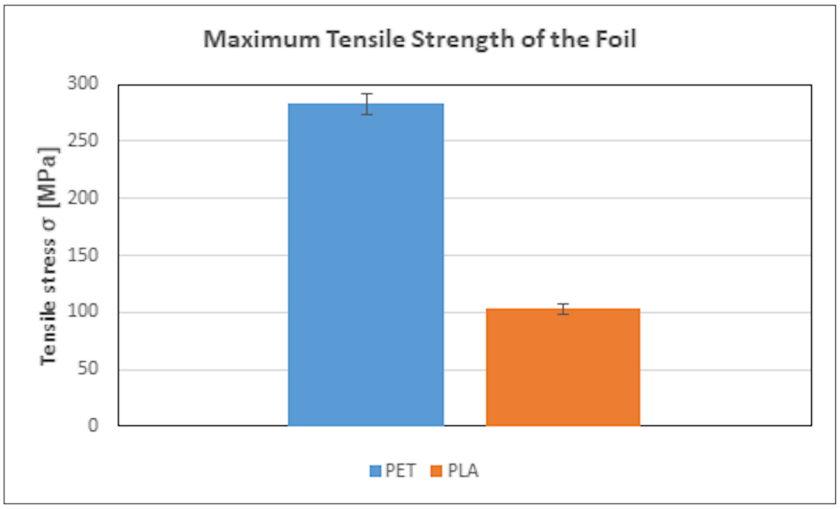

Fig. 7 Maximum tensile strength of commercial PET and PLA for a reference

comparison, the average carbon footprint of conventional PV electricity technologies is around 50 g CO_2eq./kWh [61]. However, it should be pointed out that in the tests conducted, 10% efficiency could actually not be reached in outdoor conditions. In order to reach that, a more efficient active material would be needed with an equivalent emission profile to P3HT:PCBM. It should be also noted that in outdoor conditions, structures 4–6 need an alternative bottom electrode with higher conductivity.

For indoor use, emissions ranged between 12 and 1972 g CO_2eq./kWh, thus being quite high for structures 1–3 (S4). In comparison, the GHG emission factor of electricity produced from natural gas is ca. 475 g CO_2eq./kWh and that of hard coal electricity is about 950 g CO_2eq./kWh) [62]. However, for structures 4–6 emission estimated values range between 12 and 108 g CO_2eq./kWh (except structure 6 with 3% efficiency and 10 years lifetime), thus being relatively competitive with other energy sources. Notably, the examined OPV structures 1–3 are considered more efficient in outdoor light conditions and, respectively, the structures 4–6 in indoor light conditions and/or at low light conditions. For information on CED under both indoor and outdoor conditions, see Figs. S5 and S6 (Supporting Information).

EPBT varied from 250 to 8 days for outdoor conditions with 3% production efficiency. For 5% production efficiency, the EPBT was between 150 and 5 days, whereas 10% efficiency was between 75 and 3 days. For indoor conditions, EPBTs were much higher (Table 3). However, for structures 4–6 with 5–10% efficiencies EPBTs were relatively competitive in the indoor conditions as well, ranging between 630 and 1100 days, i.e. 2–3 years.

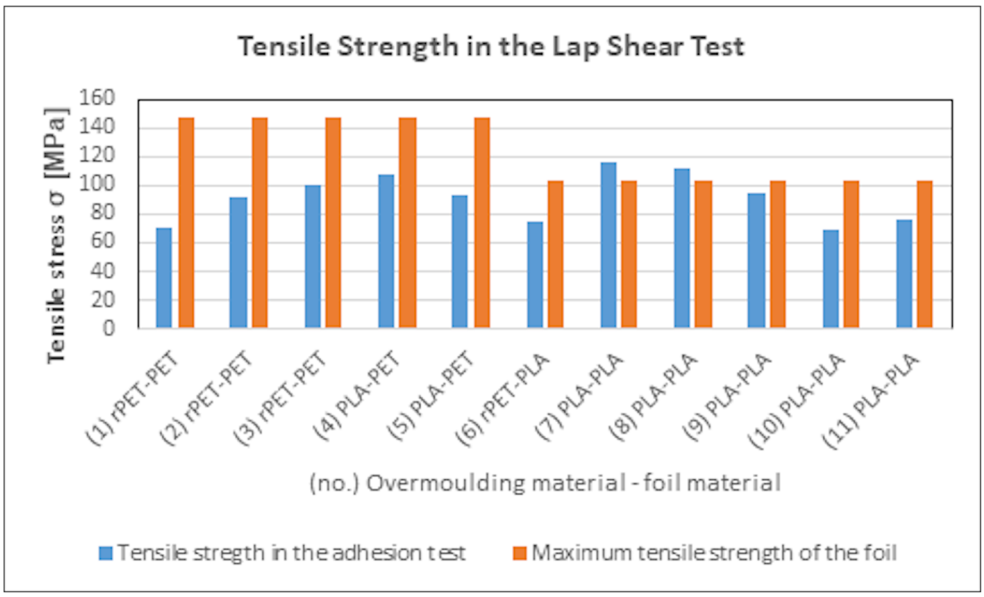

Fig. 8 Tensile strength of the foils in the lap shear test compared with the maximum tensile strength of the foils

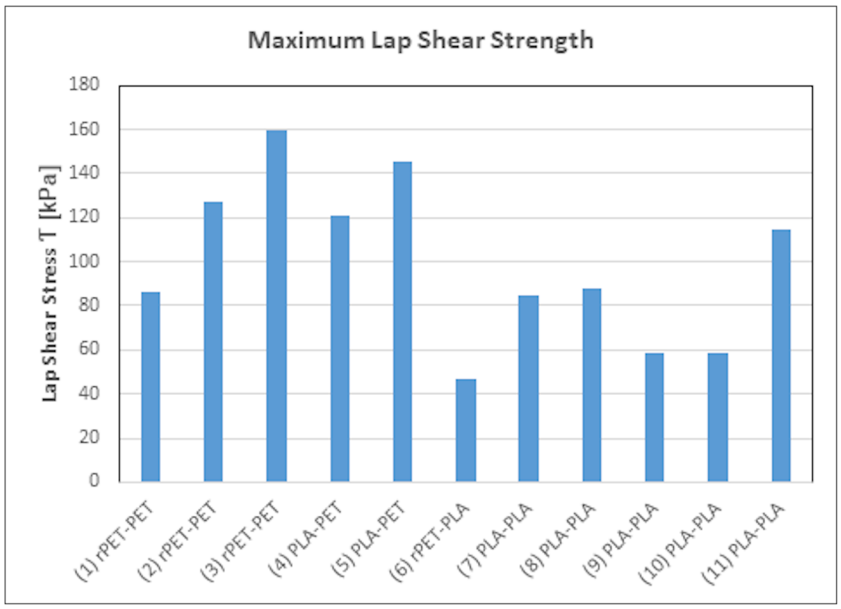

Fig. 9 Shear stress values in lap shear test

3.5 Reuse of materials

Material depletion and safety, as well as waste management, is a growing challenge. Thus, even small consumption of a depleting, toxic or hazardous material might have a huge impact globally, causing serious damage. In printed and hybrid integrated electronics devices, substrates are the main consumers of materials. Therefore, waste management/recycling processes are determined by the substrates. In all of the studied structures, a critical aspect concerning their recyclability is how easily (if at all) the different layers can be separated from one another. Another central question is whether the solar panel is integrated into another product. If this is the case, the determining factor for recycling is more likely dependent on the product in which the panel is integrated. Ag, ITO and zinc (Zn) contained in the structures 1, 2 and 3 have the most potential for recycling, particularly Ag. With increasing prices due to growing demand and more developed separation methods in the future, waste from electrical and electronic equipment could even become a source of raw materials for new products, thereby potentially making it profitable to recover these substances from the residues [63]. On the other hand, if the solar cell materials are safe and non-

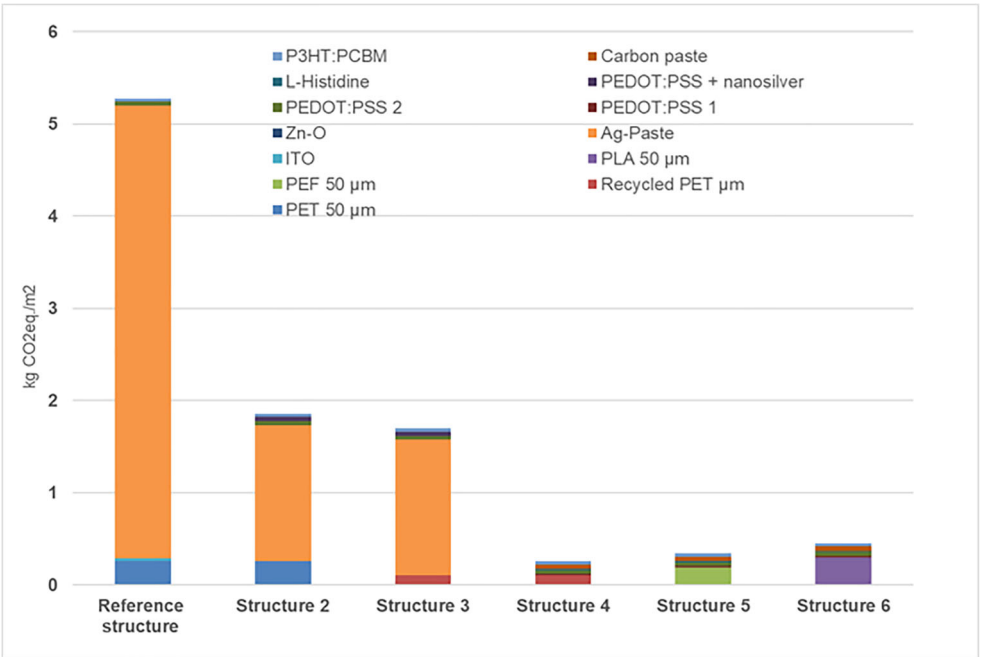

Fig. 10 Greenhouse gas emissions of the different structures in kg CO_2eq./m^2

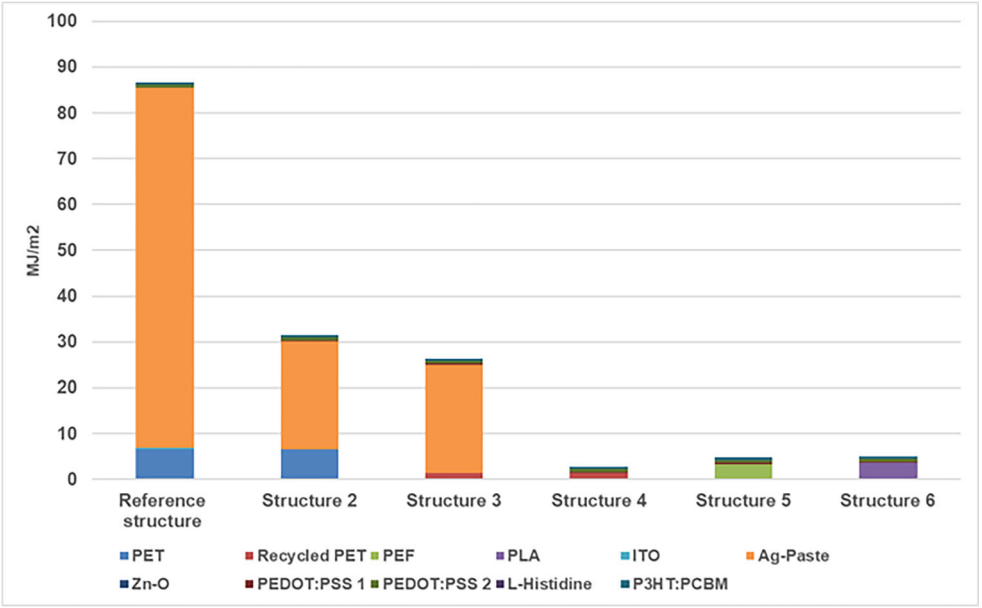

Fig. 11 Cumulative demand of fossil energy and total cumulative energy demand (including all energy sources) in MJ/m^2

hazardous, they could potentially be processed together with the substrate as part of its recycling/recovery chains.

Among the structures studied, structures 4, 5 and 6 were estimated to also have the lowest resource consumption (Table 4). Thus, they can be considered as the most compatible with the principles of a circular economy. There are no virgin fossil materials used in the substrate material, and these structures contain no metals or critical minerals either.

4 Conclusions

This study showed that printed and hybrid integrated electronics can minimize the use of virgin raw materials as well as fossil-based alternatives, resulting in increased sustainability of small electronic devices/systems and their energy systems. Herein, rPET and PLA thin films were fabricated in film extrusion process and utilized as a substrate material in printed and hybrid integrated electronics. Fabricated PLA and rPET films were compatible for printed and hybrid integrated electronics manufacturing, even for the fabrication of ultra-thin OPV structures. Scalable, energy-efficient printing technologies can replace energy-intensive vacuum processes. Gravure and screen printing of PEDOT:PSS, carbon and amino acid/heterocycles can help replacing/reducing use of metals and metal oxides. As a result, 6.9% solar cell efficiency was reached under indoor light illumination.

Higher relative adhesion of PLA-PLA interface were obtained in comparison with rPET-PET when printed and hybrid integrated LED foils were fabricated on PLA and PET films and sealed by using rPET and PLA for overmoulding. In overmoulding, the processing and handling of PLA and rPET was comparable to virgin-PET and engineering thermoplastics. The obtained results are encouraging from the point of utilization of scalable manufacturing technologies and natural/recycled materials in printed and hybrid integrated electronics.

The assessment of climate impacts, energy consumption and waste production of selected OPV structures showed that a considerable decrease in climate impacts and energy consumption can potentially be achieved through the replacement of Ag and virgin fossil-based PET. Furthermore, OPVs can potentially be used in combination with Li and other types of batteries. When

Table 3 Energy payback time in days for different efficiencies (%) in outdoor and indoor conditions

	3%, outdoors	3%, indoors	5%, outdoors	5%, indoors	10%, outdoors	10%, indoors
Reference structure	251	32,395	151	19,437	75	9719
Structure 2	91	11,787	55	7072	27	3536
Structure 3	77	9862	46	5917	23	2959
Structure 4	8	1054	5	632	2	316
Structure 5	14	1779	8	1068	4	534
Structure 6	15	1892	9	1135	4	568

Table 4 Qualitative assessment of resource consumption, recyclability and waste management of the different raw materials

Structure	Resource consumption
Reference structure	PET is based on virgin fossil-based material (crude oil). Both indium and tin are considered as critical resources [64]. Ag is also a limited resource and is often expected to be one of the main limiting factors for new energy technologies [65]. Reference structure contains Zn, which has also been listed as critical [66].
Structure 2	PET is based on virgin fossil material (crude oil). Ag is a limited resource. Structure 2 also contains Zn. The other layers are consumed in so low quantities that their contribution to the total impacts is minor.
Structure 3	The substrate in this structure is made of recycled PET material. Thus, it has a lower impact with respect to resource consumption. The main contribution to resource consumption in this structure comes from Ag and Zn.
Structure 4	In this structure, virgin fossil-based PET is replaced with recycled PET, resulting in a lower impact on resource consumptions compared with structures 2 and 3. Furthermore, this structure contains no metals.
Structures 5 and 6	Both structures 5 and 6 are made of bio-based plastics. Thus, they have higher GHG emissions and energy consumption than structure 4. However, neither of these structures contain metals. Therefore, they have a low contribution to abiotic resource consumption. There are a lot of different types of demand for bio-based materials, and their availability is therefore limited. Thus, the overall availability of bio-based plastics as replacers of fossil plastics is limited.

used in combination with OPVs, the lifetime of Li batteries could be lengthened from the present ca. 1 year to 5–10 years. By extending the battery lifetime and thereby reduce the need for new batteries, OPVs can contribute to considerable reduction in their carbon footprint and saving of Li resources.

OPV comprising rPET substrate and Ag replaced with other materials had the lowest climate impacts. Furthermore, increased lifetime and production efficiency result in a decrease of the overall environmental impact of the structures. EPBT decreased from about 250 days to less than 20 days. However, it should be noted that several sectors are interested in recycled plastics, and there is likely to be a high growth in their demand. Moreover, there is also an increasing pressure on land area resulting from both food and fuel production. Thus, there is a limit to the potential growth of these materials in the use of electronic devices. In summary, the carbon footprint and EPBT of the studied OPV structures are very low in comparison with other PV technologies, or even other renewable energy technologies. In addition, replacement of Ag and other critical minerals enable solutions that contribute to solving the challenges related to resource availability. The OPV structures produced and studied herein have a high potential of providing sustainable energy solutions for example in IoT-related technologies.

- Bio-based PLA and recycled PET films fabricated in film extrusion process are compatible for printed and hybrid integrated electronics manufacturing; PET can be replaced with PLA and rPET even in the fabrication of ultra-thin OPV structures.
- Scalable, energy-efficient printing of PEDOT:PSS, carbon and amino acid/heterocycles can help replacing/reducing use of metals, metal oxides and energy-intensive vacuum processes.
- In the overmoulding of printed and hybrid integrated LED foils, higher relative adhesion of PLA-PLA interface was obtained in comparison with rPET-PET.
- Obtained results are encouraging from the point of utilization of scalable manufacturing technologies and natural/recycled materials in printed and hybrid integrated electronics.
- Large decreases in climate impacts and energy consumption can potentially be achieved through the replacement of Ag and virgin fossil-based PET in OPV structure.
- The presented technologies could extend the lifetime of Li batteries, thereby contributing to transition to carbon-free renewable energy sources.

Acknowledgements The authors thank Tero Malm, Hannu Minkkinen and Timo Flyktman for the development work in film extrusion process; Anne Peltoniemi, Riikka Hedman and Antti Veijola for participating in the lab-scale preparation of OPVs and LED foils; Antti Veijola for the photographs; and Juha Linnekoski for providing information from PEF and Kofi Brobbey for providing valuable comments and language corrections. Part of the facilities used were provided by the Academy of Finland Research Infrastructure "Printed Intelligence Infrastructure (PIIFIRI, grant no. 320020). The work is part of the Academy of Finland Flagship Programme, Photonics Research and Innovation (PREIN), decision 320168. VTT internal funding was used to finalize the manuscript.

Funding Open access funding provided by Technical Research Centre of Finland (VTT).

References

1. EU Directive, Ecodesign, https://ec.europa.eu/growth/industry/sustainability/ecodesign_en. Accessed 1 Apr 2020
2. Evans D (2011) The internet of things: how the next evolution of the internet is changing everything. CISCO white paper, pp 1–11. https://www.cisco.com/c/dam/en_us/about/ac79/docs/innov/IoT_IBSG_0411FINAL.pdf. Accessed 1 Apr 2020
3. Pehlken A, Albach S, Vogt T (2017) Is there a resource constraint related to lithium ion batteries in cars? Int J Life Cycle Assess 22: 40–53
4. Ostfeld AE, Arias AC (2017) Flexible photovoltaic poer systems: integration opportunities, challenges and advances. Flexible and Printed Electronics 2(1):013001
5. Tuukkanen S, Välimäki M, Lehtimäki S, Vuorinen T, Lupo D (2016) Behaviour of one-step spray-coated carbon nanotube supercapacitor in ambient light harvester circuit with printed organic solar cell and electrochromic display. Sci Rep 6:22967
6. Hast J, Ihme S, Mäkinen JT, Keränen K, Tuomikoski M, Rönkä K, Kopola H (2014) Freeform and flexible electronics manufacturing using R2R printing and hybrid integration techniques, in 2014 44th European Solid State Device Research Conference (ESSDERC) 2014 Sep 22 (pp. 198–201). IEEE
7. Kololuoma T, Keränen M, Kurkela T, Happonen T, Korkalainen M, Kehusmaa M, Gomes L, Branco A, Ihme S, Pinheiro C, Kaisto I, Colley A, Rönkä K (2019) Adopting hybrid integrated flexible electronics in products: case–personal activity meter. IEEE J Electron Devi Soc 7:761–768
8. Keränen A (2016) Tactotek: fully-integrated injection molded structural electronics solutions for mass production, in Elektroniikan uudet tuulet - Tule tekemään uusia innovaatioita, Helsinki is available in Tactotek's company webpage. Tactotek Oy, TactoTek® in-mold structural electronics (IMSE™) solutions. https://tactotek.com/this-is-imse/#imse-in-a-nutshell. Accessed 15 Apr 2020
9. Meng L, Zhang Y, Wan X, Li C, Zhang X, Wang Y, Ke X, Xiao Z, Ding L, Xia R, Yip H-L, Cao Y, Chen Y (2018) Organic and solution-processed tandem solar cells with 17.3% efficiency. Science 361(6407):1094–1098
10. Lee HKH, Wu J, Barbé J, Jain SM, Wood EM, Speller EM, Li Z, Castro FA, Durrant JR, Tsoi WC (2018) Organic photovoltaic cells–promising indoor light harvesters for self-sustainable electronics. J Mater Chem A 6(14):5618–5626
11. Välimäki M, Apilo P, Po R, Jansson E, Bernardi A, Ylikunnari M, Vilkman M, Corso G, Puustinen J, Tuominen J, Hast J (2015) R2R-printed inverted OPV modules–towards arbitrary patterned designs. Nanoscale 7(21):9570–9580
12. Välimäki M, Jansson E, Korhonen P, Peltoniemi A, Rousu S (2017) Custom-shaped organic photovoltaic modules—freedom of design by printing. Nanoscale Res Lett 12(1):117–123
13. Espinosa N, Laurent A, Krebs FC (2015) Ecodesign of organic photovoltaic modules from Danish and Chinese perspectives. Energy Environ Sci 8(9):2537–2550
14. Espinosa N, García-Valverde R, Urbina A, Lenzmann F, Manceau M, Angmo D, Krebs F (2012) Life cycle assessment of ITO-free flexible polymer solar cells prepared by roll-to-roll coating and printing. Sol Energy Mater Sol Cells 97:3–13
15. Tsang MP, Sonnemann GW, Bassani DM (2016) Life-cycle assessment of cradle-to-grave opportunities and environmental impacts of organic photovoltaic solar panels compared to conventional technologies. Sol Energy Mater Sol Cells 156:37–48
16. Petritz A, Wolfberger A, Fian A, Griesser T, Irimia-Vladu M, Stadlober B (2015) Cellulose-derivative-based gate dielectric for high-performance organic complementary inverters. Adv Mater 27(46):7645–7656
17. Irimia-Vladu M, Głowacki ED, Troshin PA, Schwabegger G, Leonat L, Susarova DK, Krystal O, Ullah M, Kanbur Y, Bodea MA, Razumov VF, Sitter H, Bauer S, Sariciftci NS (2012) Indigo-a natural pigment for high performance organic field effect transistors and circuits. Adv Mater 24(3):375–380
18. Irimia-Vladu M, Głowacki ED, Voss G, Bauer S, Sariciftci NS (2012) Green and biodegradable electronics. Mater Today 15(7–8):340–346
19. Feig VR, Tran H, Bao Z (2018) Biodegradable polymeric materials in degradable electronic devices. ACS Central Science 4(3):337–348
20. Nie R, Li A, Deng X (2014) Environmentally friendly biomaterials as an interfacial layer for highly efficient and air-stable inverted organic solar cells. J Mater Chem A 2(19):6734–6739
21. Li A, Nie R, Deng X, Wei H, Zheng S, Li Y, Tang J, Wong K-Y (2014) Highly efficient inverted organic solar cells using amino acid modified indium tin oxide as cathode. Applied Physics Letters 104(12):49_1
22. Würfel U, Seßler M, Unmüssig M, Hofmann N, List M, Mankel E, Mayer T, Reiter G, Bubendorff J-L, Simon L, Kohlstädt M (2016) How molecules with dipole moments enhance the selectivity of electrodes in organic solar cells–a combined experimental and theoretical approach. Advanced Energy Materials 6(19):1600594
23. Irimia-Vladu M, Troshin P, Reisinger M, Shmygleva L, Kanbur Y, Schwabegger G, Bodea M, Schwödiauer R, Mumyatov A, Fergus J, Razumov V (2010) Biocompatible and biodegradable materials for organic field-effect transistors. Adv Funct Mater 20(23):4069–4076
24. Li W, Liu Q, Zhang Y, Li C, He Z, Choy W, Low P, Sonar P, Kyaw A (2020) Biodegradable materials and green processing for green electronics. Adv Mater 32(33):2001591
25. Sadasivuni K, Deshmukh K, Ahipa T, Muzaffar A, Ahamed M, Pasha S, Al-Maadeed M (2019) Flexible, biodegradable and recyclable solar cells: a review. J Mater Sci Mater Electron 30(2):951–974
26. MacDonald W, Looney M, MacKerron D, Eveson R, Adam R, Hashimoto K, Rakos K (2007) Latest advances in substrates for flexible electronics. J Soc Inf Disp 15(12):1075–1083
27. Choi M, Kim Y, Ha C (2008) Polymers for flexible displays: from material selection to device applications. Prog Polym Sci 33(6): 581–630
28. Khan S, Lorenzelli L, Dahiya R (2014) Technologies for printing sensors and electronics over large flexible substrates: a review. IEEE Sensors J 15(6):3164–3185
29. Espinosa N, Hösel M, Angmo D, Krebs F (2012) Solar cells with one-day energy payback for the factories of the future. Energy Environ Sci 5(1):5117–5132
30. Irimia-Vladu M, Głowacki ED, Schwabegger G, Leonat L, Akpinar HZ, Sitter H, Bauer S (2013) Natural resin shellac as a substrate and a dielectric layer for organic field-effect transistors. Green Chem 15(6):1473–1476
31. Leonat L, White M, Głowacki E, Scharber M, Zillger T, Rühling J, Hübler A, Sariciftci N (2014) 4% efficient polymer solar cells on paper substrates. J Phys Chem C 118(30):16813–16817
32. Rawat M, Jayaraman E, Balasubramanian S, Iyer S (2019) Organic solar cells on paper substrates. Advanced Materials Technologies 4(8):1900184
33. Hoeng F, Denneulin A, Bras J (2016) Use of nanocellulose in printed electronics: a review. Nanoscale 8(27):13131–13154
34. Huang J, Zhu H, Chen Y, Preston C, Rohrbach K, Cumings J, Hu L (2013) Highly transparent and flexible nanopaper transistors. ACS Nano 7(3):2106–2113
35. Chowdhury R, Nuruddin M, Clarkson C, Montes F, Howarter J, Youngblood J (2018) Cellulose nanocrystal (CNC) coatings with controlled anisotropy as high-performance gas barrier films. ACS Appl Mater Interfaces 11(1):1376–1138

36. Costa S, Pingel P, Janietz S, Nogueira A (2016) Inverted organic solar cells using nanocellulose as substrate. J Appl Polym Sci 133(28):43679
37. Gao L, Chao L, Hou M, Liang J, Chen Y, Yu H, Huang W (2019) Flexible, transparent nanocellulose paper-based perovskite solar cells. npj Flexible Electronics 3(1):1–8
38. Mattana G, Briand D, Marette A, Quintero A (2015) Polylactic acid as a biodegradable material for all-solution-processed organic electronic devices. Org Electron 17:77–86
39. Hirata M, Kimura Y (2010) Chapter 5. Structure and properties of stereocomplex-type poly(lactic acid). In: Grossman RF, Nwabunma D, Auras R, Lim LT, Selke SEM, Tsuji H (eds) Poly(lactic acid): synthesis, structures, properties, processing, and applications. JohnWiley & Sons, Inc., Hoboken, pp 449
40. Vidović E, Faraguna F, Jukić A (2017) Influence of inorganic fillers on PLA crystallinity and thermal properties. J Therm Anal Calorim 127:371–380
41. Wu J, Yen M, Wu C, Li C, Kuo MC (2013) Effect of biaxial stretching on thermal properties, shrinkage and mechanical properties of poly (lactic acid) films. J Polym Environ 21(1):303–311
42. Forrest M (2016) Recycling of polyethylene terephthalate. 331 pp. Smithers Rapra Technology, Shrewsbury
43. Apilo P, Välimäki M, Po R, Väisänen K-L, Richter H, Ylikunnari M, Vilkman M, Bernardi A, Corso G, Roesch R, Meitzner R, Schubert US, Hast J (2018) Fully roll-to-roll printed P3HT/indene-C60-bisadduct modules with high open-circuit voltage and efficiency. Solar RRL 2(3):1700160
44. Rebitzer G, Ekvall T, Frischknecht R, Hunkeler D, Norris G, Rydberg T, Schmidt W, Suh S, Weidema BP, Pennington DW (2001) Life cycle assessment: part 1: framework, goal and scope definition, inventory analysis, and applications. Environ Int 30(5):701–720
45. Lizin S, Van Passel S, De Schepper E, Maes W, Lutsen L, Manca J, Vanderzande D (2013) Life cycle analyses of organic photovoltaics: a review. Energy Environ Sci 6(11):3136–3149
46. Tsang MP, Sonnemann GW, Bassani DM (2016) A comparative human health, ecotoxicity, and product environmental assessment on the production of organic and silicon solar cells. Prog Photovolt Res Appl 24(5):645–655
47. International Organization of Standardization (ISO) (2006) Environmental Management—Life Cycle Assessment—Principles and Framework ISO 14040:2006. International Organization of Standardization, Geneva, Switzerland
48. International Organisation for Standardization (ISO) (2006) Environmental Management–Life Cycle Assessment–Requirements and Guidelines (ISO 14044). International Organisation for Standardization, Geneva, Switzerland
49. ISO TS 14067 (2013) Greenhouse Gases—Carbon Footprint of Products—Requirements and Guidelines for Quantification and Communication. International Organisation for Standardization, Geneva, Switzerland
50. Bhandari KP, Collier JM, Ellingson RJ, Apul DS (2015) Energy payback time (EPBT) and energy return on energy invested (EROI) of solar photovoltaic systems: a systematic review and meta-analysis. Renew Sust Energ Rev 47:133–141
51. Wernet G, Bauer C, Steubing B, Reinhard J, Moreno-Ruiz E, Weidema B (2016) The ecoinvent database version 3 (part I): overview and methodology. Int J Life Cycle Assess 21:1218–1230
52. Forster P, Ramaswamy V, Artaxo P, Berntsen T, Betts R, Fahey DW, Haywood J, Lean J, Lowe DC, Myhre G, Nganga J, Prinn R, Raga G, Schulz M, Van Dorland R (2007) Changes in atmospheric constituents and in radiative forcing [In: Climate Change 2007: the physical science basis. Contribution of Working Group I to the Fourth Assessment Report of the Intergovernmental Panel on Climate Change]. Cambridge University Press, Cambridge UK and New York USA
53. National Optical Astronomy Laboratory (NOAO) recommended light levels, https://www.noao.edu/education/QLTkit/ACTIVITY_Documents/Safety/LightLevels_outdoor+indoor.pdf. Accessed 15 Mar 2019
54. Ministry of the Environment D3 laskentaopas Valaistuksen tehontiheyden ja tarpeenmukaisuuden erillistarkastelut E-luvun laskennassa (in Finnish), RakMK D3 2012 mukaan, http://www.ym.fi/download/noname/%7B7912D4F8-E9C6-4E14-ADDB-81206BD007FC%7D, 2015. Accessed 15 Mar 2019
55. Steim R, Ameri T, Schilinsky P, Waldauf C, Dennler G, Scharber M, Brabec CJ (2011) Organic photovoltaics for low light applications. Sol Energy Mater Sol Cells 95(12):3256–3261
56. Cutting CL, Bag M, Venkataraman D (2016) Indoor light recycling: a new home for organic photovoltaics. J Mater Chem C 4(43):10367–10370
57. Park SY, Li Y, Kim J, Lee TH, Walker B, Woo HY, Kim J (2018) Alkoxybenzothiadiazole-based fullerene and nonfullerene polymer solar cells with high shunt resistance for indoor photovoltaic applications. ACS Appl Mater Interfaces 10(4):3885–3894
58. Cho CK, Hwang WJ, Eun K, Choa SH, Na SI, Kim HK (2011) Mechanical flexibility of transparent PEDOT: PSS electrodes prepared by gravure printing for flexible organic solar cells. Sol Energy Mater Sol Cells 95:3269–3275
59. Yang S-S, Hsieh Z-C, Keshtov ML, Sharma GD, Chen F-C (2017) Toward high-performance polymer photovoltaic devices for low-power indoor applications. Solar RRL 1:12–1700174
60. Lee HKH, Li Z, Durrant JR, Tsoi WC (2016) Is organic photovoltaics promising for indoor applications? Appl Phys Lett 108:253301
61. EU-27 Photovoltaic electricity free GABI LCA data, http://lcdn.thinkstep.com/Node/index.xhtml?stock=default. Accessed 19 Sept 2019
62. JEC - Joint Research Centre-EUCAR-CONCAWE collaboration, European Commission, Joint Research Centre, Institute for Energy and TranspWell-to-Wheels analysis of future automotive fuels and powertrains in the European context, Well-to-Tank report, Version 4a, https://iet.jrc.ec.europa.eu/about-jec/sites/iet.jrc.ec.europa.eu.about-jec/files/documents/report_2014/wtt_appendix_4_v4a.pdf, 2014. Accessed 19 Sept 2019
63. Ylä-Mella J, Pongrácz E (2016) Drivers and constraints of critical materials recycling: the case of indium. Resources 5(4):34
64. Grandell L, Lehtilä A, Kivinen M, Koljonen T, Kihlman S, Lauri L (2016) Role of critical metals in the future markets of clean energy technologies. Renew Energy 95:53–62
65. Mohr S, Giurco D, Retamal M, Mason L, Mudd G (2018) Global projection of lead-zinc supply from known resources. *Resources* 7(1):17
66. US Goverment Department of the Interior final list of critical minerals (2018) https://www.federalregister.gov/documents/2018/05/18/2018-10667/final-list-of-critical-minerals-2018. Accessed 7 Mar 2019